



Monte Carlo Based Reliability Estimation Methods in Power Electronics

Novak, Mateja; Sangwongwanich, Ariya; Blaabjerg, Frede

Published in:
2020 IEEE 21st Workshop on Control and Modeling for Power Electronics (COMPEL)

DOI (link to publication from Publisher):
[10.1109/COMPEL49091.2020.9265685](https://doi.org/10.1109/COMPEL49091.2020.9265685)

Publication date:
2020

Document Version
Accepted author manuscript, peer reviewed version

[Link to publication from Aalborg University](#)

Citation for published version (APA):
Novak, M., Sangwongwanich, A., & Blaabjerg, F. (2020). Monte Carlo Based Reliability Estimation Methods in Power Electronics. In *2020 IEEE 21st Workshop on Control and Modeling for Power Electronics (COMPEL)* (pp. 1-7). IEEE Press. <https://doi.org/10.1109/COMPEL49091.2020.9265685>

General rights

Copyright and moral rights for the publications made accessible in the public portal are retained by the authors and/or other copyright owners and it is a condition of accessing publications that users recognise and abide by the legal requirements associated with these rights.

- Users may download and print one copy of any publication from the public portal for the purpose of private study or research.
- You may not further distribute the material or use it for any profit-making activity or commercial gain
- You may freely distribute the URL identifying the publication in the public portal -

Take down policy

If you believe that this document breaches copyright please contact us at vbn@aub.aau.dk providing details, and we will remove access to the work immediately and investigate your claim.

Monte Carlo Based Reliability Estimation Methods in Power Electronics

Mateja Novak

Department of Energy Technology
Aalborg University
Aalborg, Denmark
nov@et.aau.dk

Ariya Sangwongwanich

Department of Energy Technology
Aalborg University
Aalborg, Denmark
ars@et.aau.dk

Frede Blaabjerg

Department of Energy Technology
Aalborg University
Aalborg, Denmark
fbl@et.aau.dk

Abstract—In mission-profile based reliability assessments, it is a common method to calculate the static parameters that represent the thermal stress of power electronic converters. These parameters are afterwards used in Monte Carlo (MC) simulations for estimating the expected lifetime of the components in power converters taking into account variations. However, the static parameters do not always represent the real field operating conditions of the components in power converters. To overcome this limitation, two approaches to introduce a parameter variance are implemented in the dynamic mission profile characteristics used in MC simulations in this paper. In two different application cases, it is demonstrated that using static parameters can introduce a significant error in the MC simulation. For the photovoltaic (PV) inverter applications the lifetime of a semiconductor can be overestimated up to 30% if the static parameters are used, while for uninterrupted power supply (UPS) system applications this difference can reach almost 50%.

Index Terms—Converter reliability, lifetime prediction, mission profiles, Monte Carlo methods.

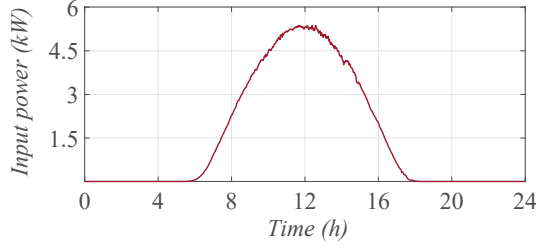
I. INTRODUCTION

The estimation of the power electronic converter reliability has gained a lot of attention both in academia and industry [1], [2]. The goal is to find the components that are most prone to failure and ensure their reliability through the design. In power electronic converters systems, the critical components to failure are the semiconductor devices and the capacitors [2]. The degradation of these components is mainly caused by the thermal stress. To obtain an accurate lifetime estimation of a power electronics converter component, the reliability analysis needs to be carried out considering a mission profile, which is a representation of the real field operating conditions of the component in power electronic converters.

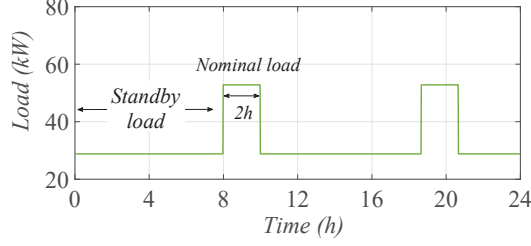
In this paper, the focus will be put on the reliability of the semiconductor device in power electronic converters. To calculate the damage due to the thermal cycling, empirical lifetime models of the devices are used [3]. Those are typically provided by the semiconductor manufacturers and they include several thermal stress parameters, like mean junction temperature (T_j), temperature swing (ΔT_j), minimum junction temperature ($T_{j\min}$), pulse duration or heating time t_{on} , and lifetime model parameters e.g. current per bond wire (I_B), bond wire diameter (D), voltage class (V_c), bond wire aspect ratio (ar), activation energy (E_a) [4], [5]. The empirical

lifetime models are often based on accelerated test results with a specific number of samples. Most lifetime models have a certain uncertainties, which originate in the variance of the semiconductor manufacturing process or the variance in the parameters that are used to fit the model. Both uncertainties should be taken into account in the lifetime estimation process. Therefore, in most mission profile-based reliability estimation methods, a variation of the model fitting parameters and mission profile parameters are usually included [6]–[8]. Since the mission profile dynamic is continuously changing during the year, a conversion of the dynamic thermal stress parameters to an equivalent static one was proposed in [9]. This approach is simple and can effectively calculate the accumulated damage distribution by applying a variation to the static values in Monte Carlo (MC) simulations. However, for a very high dynamic mission profile it might not be suitable to represent all the dynamics of a device junction temperature with one set of static parameters. This could result in an underestimated lifetime of the component. In this paper, two dynamic mission profile MC methods are used and compared to the static mission profile MC for different applications such as UPS and PV systems in order to define, how does the use of dynamic mission profile affect the estimated lifetime of the converters.

The following sections will investigate the topic of using MC analysis for two different applications: a two level inverter used in a PV application with a traditional linear controller as presented in [7] and a three-level neutral point clamped (NPC) inverter with predictive controller and active thermal control used for an uninterruptible power supply (UPS) application [10]. The two applications were chosen due to their very distinctive mission profiles shown in Fig. 1. While the PV inverter can experience high fluctuations and long loading periods in the mission profile, the UPS inverter has repetitive loading cycles with a long period of standby load and short intervals with the nominal load. Consequently, the thermal stress profile of the devices in the two applications will also be different as demonstrated in Fig. 2. For the PV inverter, it will be demonstrated how each of the MC analysis methods modifies the dynamic mission profile obtained from PV inverter test-bench. In the last section, for both applications a comparison of the estimated lifetimes is presented for different MC analysis methods and lifetime model parameter variances.

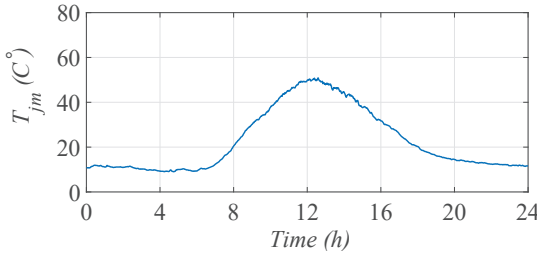


(a) PV application.

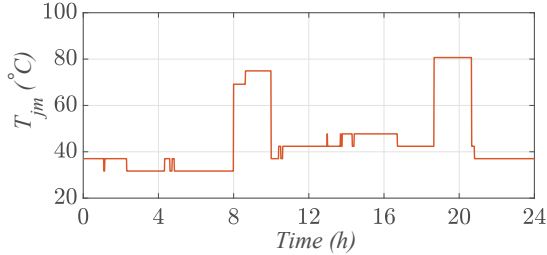


(b) UPS application.

Figure 1: Daily mission profiles used for lifetime estimation of power electronics converter devices.



(a) PV application.

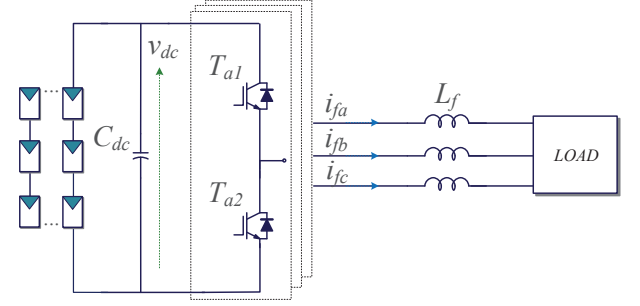


(b) UPS application.

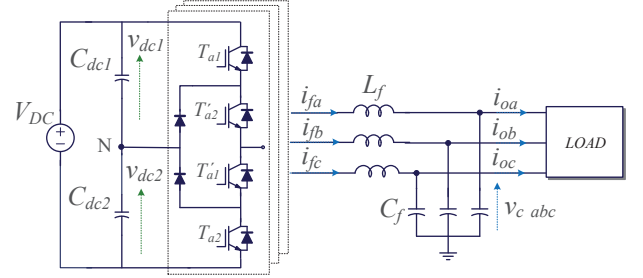
Figure 2: Daily thermal stress profiles of the IGBTs corresponding to the mission profile in Fig. 1.

II. SYSTEM CONFIGURATIONS

The Monte Carlo lifetime analysis methods will be applied to two inverter applications with different mission profiles. First application is a PV system like shown in Fig. 3a. The PV system is operating in standalone configuration with a resistive load. For extracting the maximum power from the PV array, an MPPT algorithm is used. Linear controllers are used to regulate the output current and the DC-link voltage. The system parameters, which are also used to create a Simulink model of the PV system, are given in Table I. Using the device



(a) two level inverter in PV application.



(b) 3L-NPC inverter in UPS application.

Figure 3: Inverter configuration schemes for PV and UPS applications.

Table I: Parameters of a two-level inverter in standalone PV application.

Parameter	Value
PV rated power	$P_{out} = 2.5 \text{ kW}$
Output current	$i_f = 30 \text{ A}, f_{out} = 50 \text{ Hz}$
DC-link voltage	$V_{dc} = 400 - 600 \text{ V}$
DC-link capacitance	$C_{dc} = 340 \mu\text{F}$
Output filter	$L_f = 2.5 \text{ mH}$
Load resistance	$R_{load} = 16.5 \Omega$
Switching frequency	$f_{sw} = 10 \text{ kHz}$

manufacturer datasheet [11], thermal models of the devices were created in a look-up table.

Second application, that will be used in the lifetime analysis, is an UPS system using a 3L-NPC inverter shown in Fig. 3b. The control is based on model predictive control (MPC) algorithm, which provides a simple inclusion of all control objectives and has a fast transient response. For UPS systems, the fast response to load changes and low distortion of the output voltage are out of great importance. The MPC algorithm is used to control the output voltage, the DC-link capacitor voltage balance and provide the balanced distribution of thermal stress [10]. The latter is required to ensure that the thermal stress is evenly distributed between the inner and the outer active devices, otherwise the lifetime of one pair of the devices will be much lower due to the higher applied thermal stress [12], [13]. Similar to the PV inverter, the 3L-NPC inverter is also connected to a resistive load through an

Table II: Parameters of a 3L-NPC inverter system in a UPS application.

Parameter	Value
Nominal power	$P_{out} = 53 \text{ kW}$
Output voltage	$v_c = 325 \text{ V}, f_{out} = 50 \text{ Hz}$
DC-link voltage	$V_{dc} = 700 \text{ V}$
DC-link capacitance	$C_{dc} = 4.1 \text{ mF}$
Output filter	$L_f = 2.4 \text{ mH}, C_f = 15 \text{ } \mu\text{F}$
Load resistance	$R_{load} = 3 \text{ } \Omega$
Sampling frequency	$f_{sw} = 40 \text{ kHz}$

output filter. The parameters of the UPS system are given in Table II. For obtaining the thermal model of the IGBT devices the manufacturer datasheet was used [14].

III. LIFETIME ASSESSMENT OF POWER ELECTRONIC CONVERTERS

As shown in the lifetime assessment workflow in Fig. 4, the first step is the stress analysis of the components. The stress conditions are related to the mission profile of the semiconductor devices (e.g. voltages, currents, and ambient temperature) and they are reflected in the junction temperature variation of the semiconductor devices during the operation. This is typically performed by using an electro-thermal model of the power converter system. Afterwards, the junction temperature is used to analyse the accumulated damage of the devices during the mission profile operation.

The temperature cycling occurs in the junction temperature of the devices due to the variation of the ambient temperature and loading conditions. It is required to employ a Rainflow counting algorithm to obtain the number of cycles (n_i), temperature swing ΔT_j , mean junction temperature T_{jm} and heating time t_{on} from junction temperature profile [2], [3]. The empirical lifetime model that will be used to predict the number of cycles to failure (N_f) was obtained by fitting the power cycling test results of the 5th generation IGBT devices as [4]:

$$N_f = A \cdot \Delta T_j^{\beta_1} \exp\left(\frac{\beta_2}{(T_{j,min} + 273)}\right) \cdot t_{on}^{\beta_3} \cdot I_B^{\beta_4} \cdot V_C^{\beta_5} \cdot D^{\beta_6} \quad (1)$$

where $\beta_1 - \beta_6$ are the model fitting parameters and A is the technology factor parameter. The parameter values and corresponding variance intervals can be found in [4]. After obtaining the number of cycles to failure, the lifetime consumption (LC) of the semiconductor device can be calculated using the Miner damage model (2) [3]:

$$LC = \sum_i \frac{n_i}{N_{fi}} \quad (2)$$

where n_i is the number of cycles and N_{fi} is the number of cycles to failure for the same cycle and stress type calculated from (1).

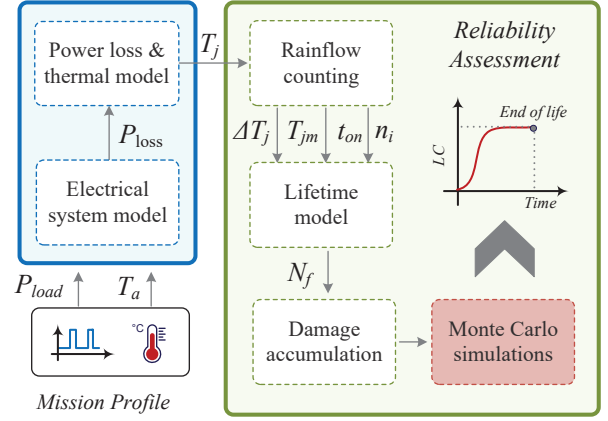


Figure 4: Workflow of the mission-profile based lifetime (LT) estimation of power converters.

IV. MONTE CARLO ANALYSIS OF POWER ELECTRONIC CONVERTERS

As discussed in the introduction, parameter variations are normally introduced during the lifetime estimation. For an empirical lifetime model in (1), that predicts the bond-wire failure for IGBTs, it can be noticed that there are several model parameters that may introduce uncertainty. For model fitting parameters (β_1 and β_2), the interval of variance is already given in [4]. The junction temperature parameters in the model will also vary. It is widely accepted that a normal distribution with a certain variation range (e.g 5%) is assumed for the lifetime model parameters representing the variations in the semiconductor device manufacturing process [8]. What can potentially make a difference in the lifetime estimation is whether this parameter variation is applied to a dynamic or to a static mission profile. Thus, three different types of MC simulations will be considered in this paper for estimating the lifetime of semiconductor devices in the PV and UPS applications:

- Monte Carlo with static parameters (MC-SP)
- Monte Carlo with semi-dynamic parameters (MC-SDP)
- Monte Carlo with dynamic parameters (MC-DP)

A. Monte Carlo with static parameters (MC-SP)

The Monte Carlo using static parameters is a conventional MC method for lifetime estimation of the semiconductor devices. It requires a conversion of the dynamic mission profile to an equivalent static profile. In the first step, using the dynamic mission profile and lifetime model (1), a lifetime consumption (LC_{dyn}) is calculated. Afterwards, using the same lifetime model, a set of static stress parameters (ΔT_j , t_{on} and $T_{j,min}$) that will result with the same LC_{dyn} value need to be found. For example $t_{on,static}$ and $T_{j,min,static}$ could be calculated as average values from the dynamic t_{on} and $T_{j,min}$. Thus, the only unknown variable in (1) will be $\Delta T_{j,static}$. After obtaining these values, a variance with normal distribution $var(m)$ is applied to the static parameters

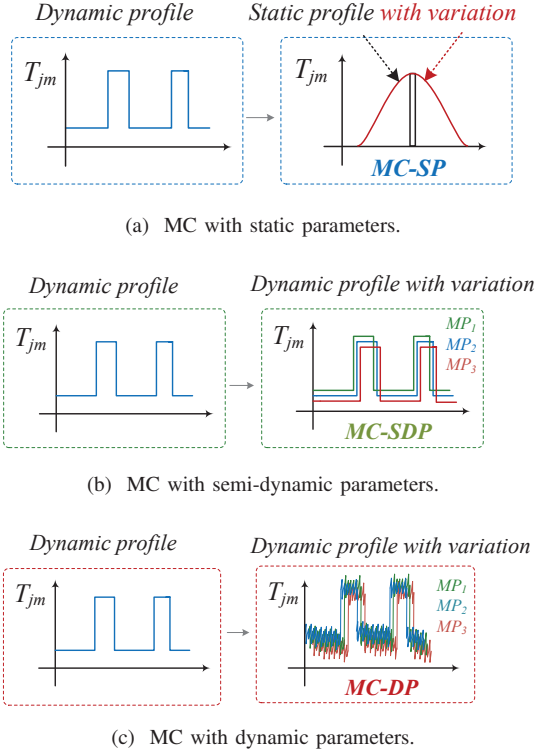


Figure 5: Conversion of the dynamic mission profile (MP) to static parameter with variance, semi-dynamic profile with parameter variance and dynamic profile with parameter variance.

$\Delta T_{j \text{ static}}$ and $T_{j \text{ min static}}$ as shown in Fig 5a. For example the distribution of $\Delta T_{j \text{ MC-SP}}$ is obtained as:

$$\Delta T_{j \text{ MC-SP}}(m) = \Delta T_{j \text{ static}} + \text{var}(m) \cdot \Delta T_{j \text{ static}} \quad (3)$$

where m is the number of MC simulations that will be conducted. In the next step, the static $\Delta T_{j \text{ MC-SP}}$ and $T_{j \text{ min MC-SP}}$ distributions are sampled using the MC method and used to calculate the distribution of the lifetime consumption (LC), which takes into account the semiconductor device parameter variations.

B. Monte Carlo with semi-dynamic parameters (MC-SDP)

The principle of applying Monte Carlo analysis with semi-dynamic parameters is as follows. In each MC simulation one sample is randomly picked from the variance distribution (e.g. from a 5% variance shown in Fig. 6) and this sample is then added to all points of the dynamic profile. As demonstrated in the example from Fig. 5b after conducting three MC simulations, the original dynamic profile $T_{j \text{ orig}}(t)$ is transformed into multiple dynamic profiles (MP_1, MP_2, MP_3) and each mission profile has a fixed variance $\text{var}_1, \text{var}_2, \text{var}_3$ that has been sampled from the normal distribution $\text{var}(m)$:

$$T_{j \text{ MC-SDP}}(m, t) = T_{j \text{ orig}}(t) + \text{var}(m) \cdot T_{j \text{ orig}}(t) \quad (4)$$

where m is the number of MC simulations that will be conducted. In other words, each MC simulation with semi-

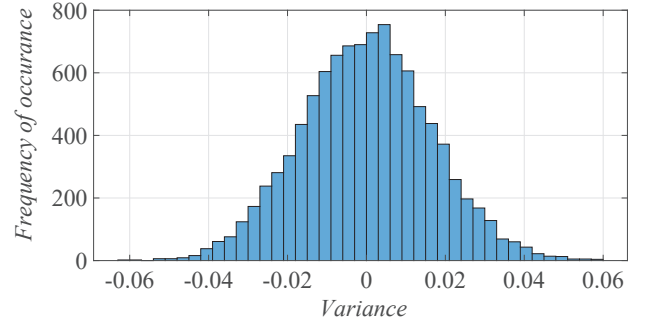


Figure 6: Example of a normal distribution for 5% variance.

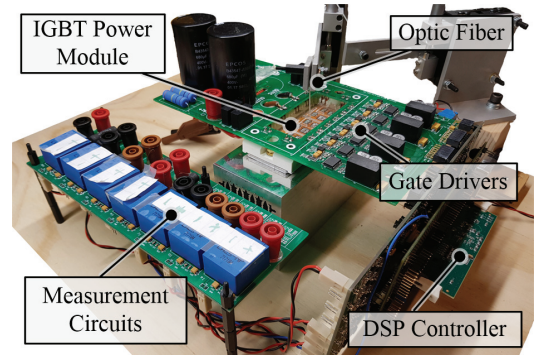


Figure 7: PV inverter test-bench used for obtaining the device thermal stress profile.

Table III: Comparison of the Monte Carlo methods.

MC method	Stress profile	Variance	Total no. of calculations
MC-SP	Time independent	Time independent	m
MC-SDP	Time dependent	Time independent	$m * t$
MC-DP	Time dependent	Time dependent	$m * t * t$

Note: m is number of MC simulations, t is number of stress profile samples

dynamic parameters has a different variance, however the variance is constant during the whole mission profile of one MC simulation. Compared to the MC with static parameters, this method does not require a conversion of the dynamic profile to the static profile but increases the number of simulations and thereby computational burden.

C. Monte Carlo with dynamic parameters (MC-DP)

The Monte Carlo analysis with dynamic parameters applies the parameter variation directly to the dynamic mission profile in the following way. For each MC simulation a normal variance distribution is generated e.g. like presented in Fig. 6. The distribution has the same number of samples as the mission profile. Next, for each sample of the dynamic mission profile, a random sample is picked out of the variance distribution and they are then added together:

$$T_{j \text{ MC-DP}}(m, t) = T_{j \text{ orig}}(t) + \text{var}(m, t) \cdot T_{j \text{ orig}}(t) \quad (5)$$

where n equals the number of samples of the dynamic mission profile. The process is then repeated for the next MC simulation. In this way all the samples of one dynamic mission profile do not have a constant variance like in MC-SDP. In Fig. 5c it can be observed how the introduced variation transforms the original dynamic mission profile into three new dynamic profiles (MP_1, MP_2, MP_3). Compared to the other MC simulation methods, the MC-DP requires the highest computational effort since it introduces the variation sample by sample. A summary of the characteristics of three MC methods is given in Table. III.

V. THERMAL STRESS ANALYSIS

In this section the impact of MC simulation methods on the dynamic mission profile will be demonstrated. The device thermal stress profile was obtained from the two-level PV inverter in the test-bench shown in Figure 7. To emulate the behaviour of PV array, the test bench is using a PV simulator. Optic fibers are attached to the IGBT chip surface as shown in Fig. 7. The junction temperature from the open module [11] is measured and recorded using the signal conditioner.

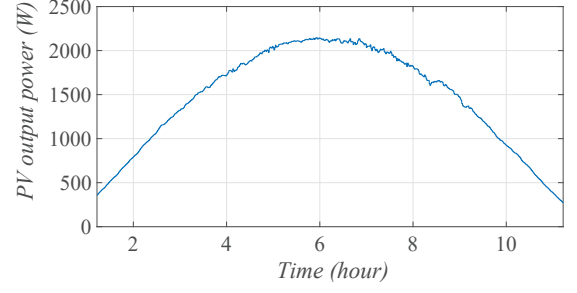
In the experiments, PV simulator was programmed to emulate the behaviour of the PV array during a clear day (see Fig. 8) and also during a cloudy day (see Fig. 9). The corresponding device junction temperatures can also be observed for a clear day and a cloudy day, respectively. For the cloudy day, the fluctuation in the energy production from the PV array will cause high temperature swings. If a constant variation of 2%, 0% and 5% are applied to the mission profile like this is performed in MC with semi-dynamic parameters (MC-SDP), the mission profiles from Fig. 8 and Fig. 9 will be transformed to profiles shown in Fig. 10. On the other hand if instead of a fixed variation, a normal distribution with standard deviation of 5% is applied like in MC with dynamic parameter (MC-DP), the mission profiles will look like in Fig. 11. It can be seen that the MC-DP adds an additional dynamic to each mission profile measurement compared to the original dynamic profile without the parameter variance.

VI. END-OF-LIFE DISTRIBUTION ANALYSIS

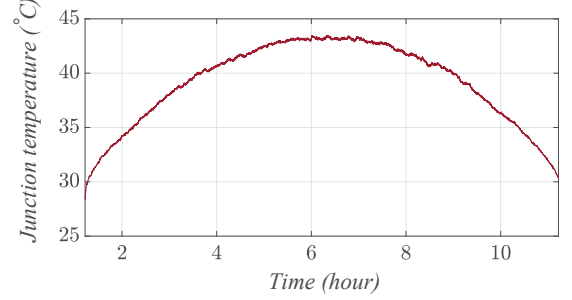
Using the MC simulations introduced in the previous section, the end-of-life cumulative distribution function (*cdf*), i.e. the unreliability function for the PV inverter devices and the UPS inverter devices can be obtained. Afterwards, the device *cdf* functions can be used to calculate the unreliability function $F_{sys}(x)$ for the inverter. For the two level inverter in PV application, the $F_{sys}(x)$ is calculated as:

$$F_{sys}(x) = 1 - (1 - F_{T_1}(x))^6 \quad (6)$$

where $F_{T_1}(x)$ is the *cdf* of IGBT device in the two level inverter. In this topology the loading conditions in each phase are equivalent. Therefore, the *cdf* functions of the $F_{T_1}(x)$ can be raised to the power of 6. For the 3L-NPC inverter in the UPS application there are two pairs of IGBT devices that are

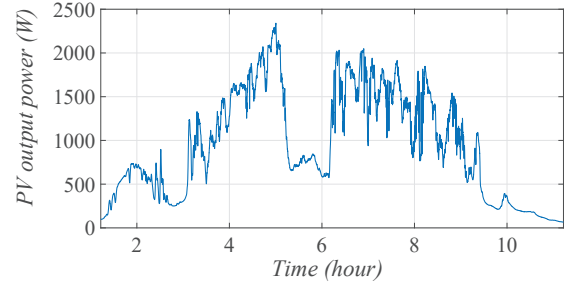


(a) PV array output power.

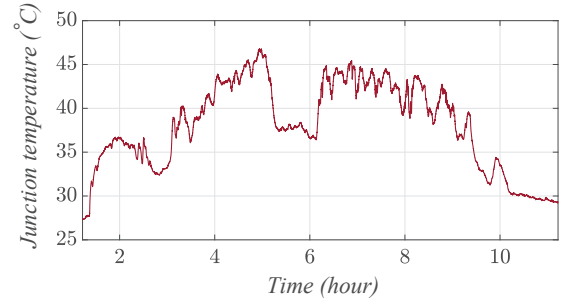


(b) PV inverter IGBT device junction temperature.

Figure 8: Daily mission profile of a PV inverter for a clear day.



(a) PV array output power.



(b) PV inverter IGBT device junction temperature.

Figure 9: Daily mission profile of a PV inverter for a cloudy day.

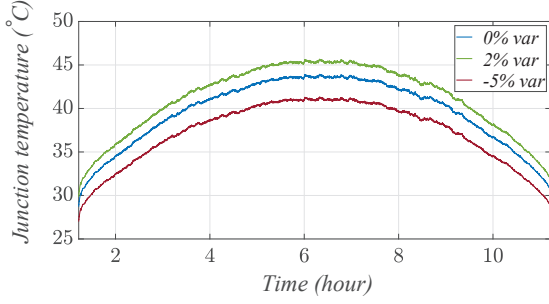
experiencing the same thermal stress conditions. The $F_{sys}(x)$ for the 3L-NPC inverter can be defined:

$$F_{sys}(x) = 1 - (1 - F_{T_1}(x))^6 (1 - F_{T_2'}(x))^6 \quad (7)$$

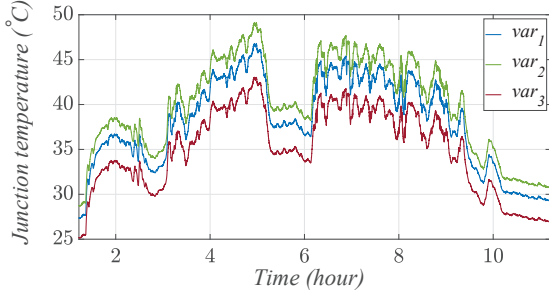
where $F_{T_1}(x), F_{T_2'}(x)$ are the unreliability functions of the inner and outer IGBT devices. It is assumed that the NPC

Table IV: B_1 and B_{10} lifetime estimation (years) for different parameter variations in Monte Carlo simulations.

MC simulation methods	MC-SP			MC-SDP			MC-DP		
Parameter variation	1%	5%	10%	1%	5%	10%	1%	5%	10%
B_1 (UPS application)	9.82	9.02	8.01	6.81	6.61	5.81	6.21	4.01	2.40
B_{10} (UPS application)	25.25	23.85	22.04	19.84	19.63	17.84	18.24	11.62	7.21
B_1 (PV application)	12.83	12.63	11.42	9.02	8.81	7.82	8.62	7.82	6.01
B_{10} (PV application)	34.47	34.07	32.26	28.06	27.65	25.85	27.05	24.25	19.04



(a) Clear day.



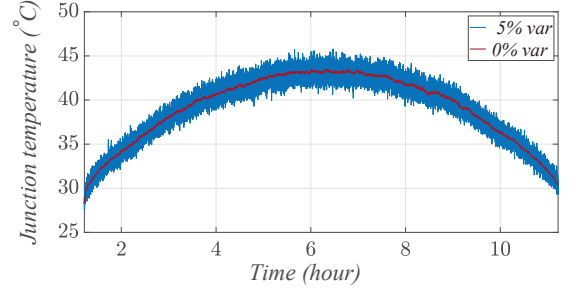
(b) Cloudy day.

Figure 10: Dynamic junction temperature profiles in Monte Carlo method with semi-dynamic parameters (MC-SDP).

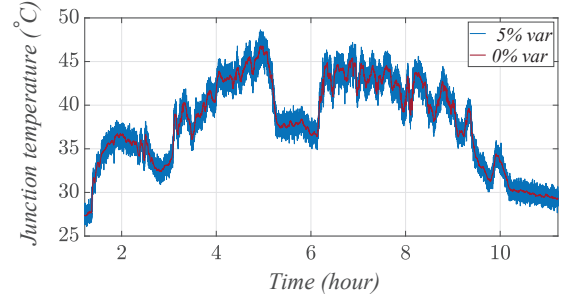
system will fail if one of the 12 devices fails. Due to unidirectional power flow of both applications in this paper, the diodes are not experiencing any high thermal loading like the IGBT devices. Therefore, the analysis is simplified to only include the active devices, which significantly contribute to the lifetime consumption of the inverters.

For both applications, a population of 10 000 devices was used in the three MC methods. Among the three MC methods the MC-SP is the fastest method and MC-DP is the slowest. To illustrate the execution time, the MC-SP was executed in 1 second for the PV application, which had a mission profile of almost 104 000 samples, while the MC-DP needed 300 seconds. In Fig. 12a a lifetime model parameter variation of 5% the *cdf* plots for the PV inverter can be observed. All three MC methods showed different unreliability functions. The MC-SP results in the longest expected lifetime, while the MC-DP results in the shortest. Similar trends were also observed for the UPS inverter in Fig. 12b.

One of the commonly used metrics in the lifetime analysis is the B_x lifetime i.e. the time when $x\%$ of the device population



(a) Clear day.



(b) Cloudy day.

Figure 11: Dynamic junction temperature profile in Monte Carlo method with dynamic parameters (MC-DP).

have failed. In Fig. 12, B_1 and B_{10} lifetime, are highlighted [15]. The MC simulations for the two applications were also repeated for model parameter variation of 1% and 10%. The expected B_1 and B_{10} lifetimes for all cases are summarized in Table IV. If the B_{10} lifetimes obtained using the MC-SP for PV inverter and UPS inverter are compared to the MC-SDP a 18% difference can be noticed. In the comparison to the MC-DP, this difference is even larger as shown in Fig. 13.

VII. CONCLUSION

A comparison of three different MC analysis methods used for lifetime estimation of power electronic converters is presented in this paper. The use of MC simulation with dynamic parameters has the highest impact on the estimated lifetime. This type of MC simulation is more time-consuming than the MC simulation with static parameters. However, the error in the estimated B_{10} lifetime can be as high as 30% for the PV inverter application if a 5% parameter variation is used in the lifetime model, and this is important to consider in the analysis phase. For the UPS application the error is

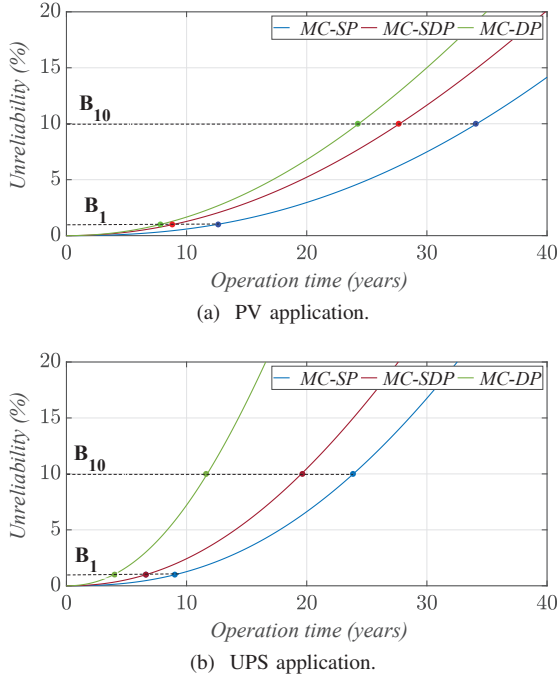


Figure 12: Comparison of unreliability functions for 5% lifetime model parameter variation using static parameters (MC-SP) and dynamic parameters (MC-SDP and MC-DP) in the Monte Carlo analysis.

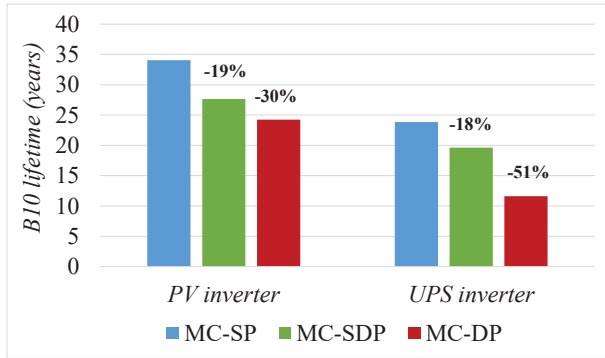


Figure 13: Expected B_{10} lifetime for the PV and UPS inverter with 5% lifetime model variance.

even larger and can reach almost 50%. Therefore, if static parameters are used in the MC lifetime analysis of the power converter devices, we have to be aware that parameter variance will not be captured in the same measure.

ACKNOWLEDGEMENT

The work is supported by the Reliable Power Electronic-Based Power System (REPEPS) project at the Department of Energy Technology, Aalborg University as a part of the Villum Investigator Program funded by the Villum Foundation.

REFERENCES

- [1] F. Richardeau and T. T. L. Pham, "Reliability calculation of multilevel converters: Theory and applications," *IEEE Trans. Ind. Electron.*, vol. 60, no. 10, pp. 4225–4233, Oct 2013.
- [2] K. Ma, H. Wang, and F. Blaabjerg, "New approaches to reliability assessment: Using physics-of-failure for prediction and design in power electronics systems," *IEEE Power Electron. Mag.*, vol. 3, no. 4, pp. 28–41, Dec 2016.
- [3] Z. Ni et al., "Overview of real-time lifetime prediction and extension for SiC power converters," *IEEE Trans. Power Electron.*, vol. 35, no. 8, pp. 7765–7794, 2020.
- [4] R. Bayerer, T. Herrmann, T. Licht, J. Lutz, and M. Feller, "Model for power cycling lifetime of IGBT modules - various factors influencing lifetime," in *Proc. of CIPS*, 2008, pp. 1–6.
- [5] U. Scheuermann, R. Schmidt, and P. Newman, "Power cycling testing with different load pulse durations," in *Proc. of PEMD 2014*, 2014, pp. 1–6.
- [6] V. Raveendran, M. Andresen, and M. Liserre, "Improving onboard converter reliability for more electric aircraft with lifetime-based control," *IEEE Trans. Ind. Electron.*, vol. 66, no. 7, pp. 5787–5796, 2019.
- [7] A. Sangwongwanich, Y. Yang, D. Sera, and F. Blaabjerg, "Mission profile-oriented control for reliability and lifetime of photovoltaic inverters," *IEEE Trans. Ind. Appl.*, vol. 56, no. 1, pp. 601–610, Jan 2020.
- [8] P. D. Reigosa, H. Wang, Y. Yang, and F. Blaabjerg, "Prediction of bond wire fatigue of IGBTs in a PV inverter under a long-term operation," *IEEE Trans. Power Electron.*, vol. 31, no. 10, pp. 7171–7182, 2016.
- [9] J. W. Mcpherson, *Reliability Physics and Engineering: Time-To-Failure Modeling*, 3rd ed. Springer International Publishing, 2019.
- [10] M. Novak, T. Dragicevic, and F. Blaabjerg, "Finite set MPC algorithm for achieving thermal redistribution in a neutral-point-clamped converter," in *Proc. of IECON 2018*, Oct 2018, pp. 5290–5296.
- [11] *FS50R12KT4 B15 datasheet*, Infineon Technologies AG, 2009, rev. 3.0.
- [12] J. Rodriguez, S. Bernet, P. K. Steimer, and I. E. Lizama, "A survey on neutral-point-clamped inverters," *IEEE Trans. Ind. Electron.*, vol. 57, no. 7, pp. 2219–2230, July 2010.
- [13] M. Novak and F. Blaabjerg, "Model predictive active thermal control strategy for lifetime extension of a 3l-npc converter for ups applications," in *Proc. of COMPEL*, 2020, pp. 1–7.
- [14] *3-Level NPC IGBT-Module: SKiiP 28MLI07E3V1 datasheet*, Semikron, 6 2016, rev. 1.0.
- [15] *Load-cycling capability of HiPak IGBT modules.*, Berner, J, 2012, 201.